Periodontal ligament stem cells inhibit THP-1 macrophage pyroptosis via modulating the NF-κB/NLRP3/GSDMD signaling axis

Wenxuan Wang (xgzd1127@163.com)
The Affiliated Hospital of Qingdao University
Chun Fan
The Affiliated Hospital of Qingdao University
Xinbo Yu
The Affiliated Hospital of Qingdao University
Xu Qiu
The Affiliated Hospital of Qingdao University
Yingzhe Hu
The Affiliated Hospital of Qingdao University
Shuhan Li
The Affiliated Hospital of Qingdao University
Xiangru Gao
The Affiliated Hospital of Qingdao University
Qiuxia Ji
The Affiliated Hospital of Qingdao University

Research Article

Keywords: PDLSCs, Macrophage, NLRP3 inflammasome, GSDMD, Pyroptosis, Periodontitis.

Posted Date: July 18th, 2022

DOI: https://doi.org/10.21203/rs.3.rs-1851176/v1

Abstract

Background: To investigate the pathological crosstalk between pyroptosis and periodontitis by addressing the following questions: 1) Does pyroptosis play any pathobiological roles in the onset and progression of periodontitis?; 2) Are the localized periodontal macrophages major cell type in pyroptosis?; 3) Can *in vitro* stimulation by *Porphyromonas gingivalis*-derived lipopolysaccharide (*P.g*-LPS) and adenosine triphosphate (ATP) in THP-1 macrophages induce pyroptosis via activation of the NF-κB/NLRP3/GSDMD signaling axis?; and 4) Is there any paracrine effect of periodontal ligament stem cells (PDLSCs) on the NF-κB/NLRP3/GSDMD pathway in pyroptosis?

Methods: Clinical periodontitis tissue samples were collected from voluntarily enrolled participants who visited the Dental Clinic of the Affiliated Hospital of Qingdao University. *In vitro*, THP-1 macrophage pyroptosis was induced by treating with *P.g*-LPS in combination with ATP. The qRT-PCR, western blotting, and ELISA methods were used to determine the expression levels of NF-κB, NLRP3, caspase-1, ASC, GSDMD, IL-1β, and IL-18. We used the 2 ,7 -dichlorodihydrofluorescein diacetate fluorescence probe to measure ROS levels in THP-1 cells. The caspase-1 activity assay, cytotoxicity assay, and double staining with Hoechst 33342 and propidium iodide were performed in pyroptotic THP-1 macrophages to test the paracrine effect of human PDLSCs on pyroptosis.

Results: High expressions of the canonical pyroptosis-associated factors were detected in periodontitis gingival tissues from patients compared to the healthy controls. *P.g*-LPS treatment exhibited significant stimulation of the canonical pyroptotic effectors, including NF-κB, NLRP3, caspase-1, GSDMD-N, IL-1β, and IL-18 at both mRNA and protein levels. Furthermore, induction of pyroptosis drastically increased the caspase-1 activity, the release of lactate dehydrogenase, and the percentage of cells with damaged membranes, but these pathological effects could be ameliorated via paracrine effects of PDLSCs.

Conclusions: Macrophage pyroptosis is an important contributor to the development of periodontitis, while PDLSCs can significantly attenuate the pyroptosis process induced by *P.g*-LPS/ATP by inhibiting the NF-κB/NLRP3/GSDMD signaling through its paracrine effects *in vitro*. These evidences cumulatively confirm the immunomodulatory roles of PDLSCs in periodontitis and may be exploited as an effective therapeutic target.

Introduction

Periodontitis is an inflammatory gum disease caused by periodontal bacteria and may lead to damage to gum tissues and jawbone, as well as premature loss of teeth near the affected gum areas, thus negatively impacting oral functions and quality of life[1–2]. Several gram-negative bacteria, including *Porphyromonas gingivalis*, *Aggregatibacter actinomycetemcomitans*, and *Fusobacterium nucleatum*, have been linked to periodontitis. However, *Porphyromonas gingivalis* (*P. gingivalis*) is considered the major etiopathological factor of periodontitis[3–4]. Recently, studies have revealed a causal linkage between the *P. gingivalis*-associated periodontitis and systemic diseases, such as cardiovascular disease,

diabetes and rheumatoid arthritis[5–7]. Nevertheless, the underlying pathomechanism of heightened inflammatory responses in periodontitis, leading to severe gum and teeth damage, remains unresolved.

Pyroptosis, a type of lytic inflammatory programmed cell death, is marked by the swelling and rupture of cell membranes, thereby releasing the cellar content, including inflammatory cytokines such as interleukin-1β and − 18 (IL-1β, IL-18), in the extracellular space[8–10]. The caspase-1, a member of the cysteine-dependent aspartate-directed proteases, plays essential role in the canonical pyroptosis pathway, whereas caspases-4, 5 & 11 participate in the non-canonical pathway. All the pyroptosis-related caspases mediate the lytic cell death essentially by cleavage-induced activation of gasdermin-D (GSDMD), a pore-forming cell death execution factor[11–13]. Notably, bacterial infection-induced assembly of the canonical NOD-like receptor family pyrin domain-containing protein 3 (NLRP3) inflammasome acts as a critical mediator of caspase-1 activation and the resultant extracellular secretion of proinflammatory cytokines like IL-1β and IL-18[14]. Although several studies have investigated the relationship between the induction of pyroptosis and systemic inflammation or periosteal diseases[15–17], no specific mechanism of action could be delineated so far.

The multi-protein complex NLRP3 inflammasome, composed of NLRP3, apoptosis-associated speck-like protein containing a CARD (ASC), and caspase-1[18], plays pivotal roles in sensing the pathogen-associated molecular patterns (PAMPs) following pathogenic infections, as well as the damage-associated molecular patterns (DAMPs) produced under endogenous stress conditions[19]. Gram-negative bacteria *P. gingivalis* uses the external membrane component LPS to exert its virulence effects and induce the innate immune response in the host body[20–21]. Binding of LPS to TLR4 receptor protein triggers a cascade of inflammatory signal transduction through the nuclear translocation of downstream effector NF-κB[22]. The extracellular stimuli like pathogens and ATP can activate NLRP3 inflammasomes via NF-κB-dependent priming of pro-IL-1β and NLRP3 productions to induce a myriad of cellular stress response mechanisms, including lysosomal permeability, potassium efflux, and mitochondrial reactive oxygen species (ROS) generation[19]. In support of this cellular phenomena, both NF-κB inhibitors and ROS scavengers have been shown to suppress the NLRP3 gene activation during LPS-induced immune modulation, suggesting critical epigenetic regulatory functions of ROS and NF-κB in NLRP3 expression under stress conditions[23–24].

Macrophages are heterogeneous populations of immune cells that play central roles in inflammation, immune regulation, and tissue homeostasis, which have physiological importance. However, over-production of cytokines by macrophages due to persistently activated inflammatory signaling could be detrimental, leading to acute and chronic inflammatory diseases such as arthritis, atherosclerosis, asthma, or even death[25–28]. Whether such macrophagic cytokine storm could be the underpinning of periodontitis pathogenesis has not been investigated in detail. Recently, allogeneic human periodontal ligament-derived stem cells (hPDLSCs) are mainly used for the cell therapy-based curing of periodontitis[29]. A growing body of evidence has shown that hPDLSCs have the potential to promote bone regeneration by accelerating the processes of osteoinductive signaling, accumulation of osteocytes

and cementum at the break sites, and finally bone remodeling; and also the periodontal tissue regeneration by forming new periodontal ligaments[30–31]. It has been demonstrated that hPDLSC-derived exosomes act as the signal regulator of immune activation as well as alleviate inflammation in periodontitis[32], by a yet unknown mechanism.

Therefore, this study was designed to investigate whether: 1) pyroptosis plays any pathological roles in the development and progression of periodontitis; 2) localized periodontal macrophages are the major cell type in pyroptosis; 3) *in vitro* stimulation by *P.g*-LPS and ATP in THP-1 macrophages can induce pyroptosis via activation of NF-κB/NLRP3/GSDMD signaling axis; and 4) there is any paracrine effect of PDLSCs on the NF-κB/NLRP3/GSDMD pathway during pyroptosis.

Materials And Methods

Materials

Dulbecco's modified Eagle medium (DMEM), phosphate-buffered saline (PBS), Penicillin-Streptomycin (PS) solution, trypsin and adipogenic/osteogenic induction differentiation medium were obtained from Procell (China). Fetal bovine serum (FBS) were purchased from Biological Industries (Israel). Standard preparation of *P.g*-LPS was purchased from InvivoGen (USA). ATP, phorbol myristate acetate (PMA), Cell Counting Kit-8 (CCK-8) assay were provided by MedChemExpress (USA). A ROS Fluorescence Assay Kit and Human IL-1β/IL-18 ELISA Kit were supplied by Elabscience (China). A CytoTox 96® Non-Radioactive Cytotoxicity Assay kit was purchased from Promega (USA). A Caspase-1 Activity Assay Kit was obtained from Beyotime (China). Crystal violet stain solution, paraformaldehyde (PFA)-phosphate buffer solution, bovine serum albumin (BSA), Hoechst 33342/propidium iodide (PI) double staining kit were purchased from Solarbio (China). RNAiso Plus, a PrimeScript™ RT Reagent Kit with gDNA Eraser, and TBGreen® Premix Ex Taq™ II were purchased from Takara (Japan). PCR Primers were provided by Sangon Biotech (China). All other reagents were analytical grade and were used as received without further purification.

Gingival tissue sampling and immunohistochemical (IHC) analysis

In this study, gingival tissue samples were collected from enrolled volunteer participants (age range: 25–45 years) who visited the Dental Clinic of the Affiliated Hospital of Qingdao University. Participants were distributed into two groups, the healthy control group involving 10 subjects; and the diseased group of 10 patients diagnosed with chronic inflammatory periodontal disorder. All participants were free of any systemic diseases. After collection, specimens were fixed with 4% PFA for 24 h, followed by paraffin embedding. Histological sections were cut, dehydrated, and then incubated at 4℃ overnight with anti-GSDMD (absin, China) and anti-CD68 (Elabscience, China) antibodies. Similarly, we performed an IHC with the same set of samples by co-staining with anti-GSDMD and anti-CD68 antibodies, followed by incubation with corresponding secondary antibodies. Finally, slides were scanned using the Pannoramic DESK (3DHISTECH Ltd., Hungary) imaging system, equipped with the CaseViewer software (3DHISTECH

Ltd.) for slide viewing and histopathological diagnosis. Other aliquots of gingival tissues were processed for total RNA extraction.

Isolation and culture of hPDLSCs

Periodontal ligaments were acquired from 6 healthy contributors (15–25 years old) who underwent tooth extraction due to orthodontic symptoms or having wisdom teeth. PDLSCs were gained by the tissue block method following the previously reported method[33]. Briefly, each clinically extracted tooth sample was aseptically placed in a 15ml centrifuge tube filled with DMEM, and transferred to the pathology laboratory. Sterile PBS added with 10% PS was freshly prepared for washing samples 6–7 times. Therewith, the periodontal ligament tissue in the middle 1/3rd of the root was scraped and minced into $1mm^3$ pieces using a sterile surgical knife. Then, the tissue pieces were cultured in DMEM supplemented with 20% FBS, and 1% PS in flasks at 37°C in a humidified incubator at 5% CO_2. The culture medium was changed every 3 days. When PDLSCs started to proliferate and spread around the tissue block in adherent culture, cells were passaged by trypsinization and seeded onto 10cm dishe. Then cells were cultured in DMEM medium supplemented with 10% FBS. The third to fifth passage cells were harvested for the downstream applications.

Identification of hPDLSCs

Colony-forming assay

PDLSCs were counted on a standard cell counter, and 500 cells were seeded in each well of 6-well plates for the colony forming assay. After 2 weeks, culture media were removed, and cells were rinsed thrice with PBS and fixed with 4% PFA in PBS solution for 30min, immediately followed by staining with 0.1% crystal violet solution for 15min. After that, petri dishes were rinsed with PBS three times, and colonies were counted under a light microscope.

Flow cytometric analysis

The surface markers of hPDLSCs were analyzed using flow cytometry. After trypsinization, centrifugation, and washing, from each sample, approximately $1x10^6$ singlet cells were resuspended in PBS with 1% BSA, and incubated in the dark at 4°C for 30min with FITC-conjugated monoclonal antibodies against human CD45(Elabscience, China), CD29(Elabscience, China), CD73(Elabscience, China), CD90(Thermo, Finland) and CD105(Biolegend, USA) marker proteins. After the incubation, cells were pelleted down, washed with PBS containing 1% BSA, and subjected to flow cytometric analysis.

Multilineage differentiation

To measure osteogenic differentiation, $1x10^5$ PDLSCs were seeded in each well of 6-well plates and cultured to 70% confluency. Afterward, cells were cultured in the osteogenic differentiation medium. After 21 days, cells were stained with alizarin red S to identify the population of calcium-containing osteocytes. To measure the extent of adipogenic differentiation, cells were seeded on 6-well plates in the same way.

The growth medium was changed to an adipogenic differentiation medium at the optimal cell confluency, as instructed in the manufacturer's protocol. The adipogenic effect was examined after 28 days.

Culture and pyroptosis-induction in THP-1 cells

THP-1 cells were seeded on 6-well plates at a density of $1.5x10^6$ cells per well and cultured in DMEM medium supplemented with 100ng/ml of PMA for 24h to induce adherence. Then, cells were treated with different concentrations (0.1, 1, 10μg/ml) of *P.g*-LPS for 11h, followed by 5mM of ATP for 1h. Cell viabilities under different stimulation conditions were measured by Cell CCK-8. Total RNA and protein were extracted in parallel from each treatment group for subsequent gene expression and western blot analyses.

Transwell coculture assay

First, THP-1 cells were seeded in the lower 6-well transwell chamber and treated with 10μg/ml of *P.g*-LPS and 5mM of ATP. Then, PDLSCs were seeded on the upper chamber at $1x10^5$ cells per well and cultured in DMEM medium containing 10% FBS and 1% PS. Once cells reached a confluency of 80–90% and pyroptosis was successfully induced, the transwell coculture was performed in a serum-free DMEM medium for 24h. Four different treatment groups were set: single-culture control (SCC), single-culture pyroptosis (SCP), coculture control (CCC), and coculture pyroptosis (CCP) groups.

Quantitative Real-Time PCR (qRT-PCR) assay

The total RNA from tissues and THP-1 cells was extracted using the TRIzol reagent, according to the manufacturer's instructions. The cDNA was synthesized using PrimeScript RT Master Mix (Takara) or MiX miRNA First Strand Synthesis kit (Takara). The SYBR Green PCR kit (Takara) and LightCycler 480 system were used for the quantitative mRNA expression analysis. The qRT-PCR thermal profile was as follows: 1 cycle at 95℃ for 30min in stage 1; 40 cycles at 95℃ for 5s, and 60℃ for 20s in stage 2; 1 cycle at 95℃ for 5s, 60℃ for 1 min, and 95℃ for 5s in stage 3. The glyceraldehyde 3-phosphate dehydrogenase (GAPDH) served as the internal reference. All primers were synthesized by Sangon Biotech (Table 1, China). 2-ΔΔCt method was used to calculate relative expressions of target genes.

Western blot analysis

The total protein from tissues and THP-1 cells were extracted using 1x RIPA buffer (Solarbio, China), and protein concentration was determined using the BCA kit (Elabscience, China), as directed by the manufacturer. Then protein samples were resolved in 10% SDS-PAGE gel (Elabscience, China) and electro-transferred to methanol-activated polyvinylidene difluoride (PVDF) membranes. The membranes were blocked with 5% non-fat skim milk for 2h at room temperature prior to incubation with anti-NF-κB (Abcam, UK), anti-NLPR3 (Abcam, UK), anti-caspase-1 (absin, China), anti-ASC (Abcam, UK), anti-GSDMD (novusbio, USA), and anti-IL-1β (Abcam, UK) (all diluted at 1:1000) antibodies at 4℃ overnight. The membranes were washed with tris-buffered saline-Tween 20 (TBST) buffer (Elabscience, China) three times (10min each), and then incubated with corresponding secondary antibodies (Elabscience, China) (1:10000) for 2h at room temperature, followed by washing with TBST twice (10 min each) and

developed using enhanced chemiluminescence (ECL) reagent (Elabscience, China). Relative protein levels were measured by normalizing with GAPDH using the ImageJ software (Media Cybernetics, Rockville, MD, USA).

Caspase-1 activity assay

In this assay, the ability of caspase-1 to change Acetyl-Tyr-Val-Ala-Asp p-nitroaniline (Ac-YVAD-pNA) into yellow formazan was measured. Total protein was isolated from THP-1 cells on a 96-well microtiter plate and incubated with Ac-YVAD-pNA for 2h at 37°C. A spectrophotometer was used to measure the absorbance at 405nm. Dilutions of the standards of p-nitroaniline (pNA) were used to produce the standard curve for the assay. According to the manufacturer's instructions, protein concentrations were determined by the Bradford protein assay. The caspase-1 activity was measured by determining the pNA content in each sample with respect to the standard curve.

Hoechst 33342 and PI double staining

Double staining with Hoechst 33342/PI indicated the populations of apoptotic and necrotic cells. *P.g*-LPS and ATP-treated THP-1 cells were cocultured to certain confluency, then cell culture media was thoroughly aspirated. Following the manufacturer's instructions, 5μl of Hoechst 33342, 5μl of PI, and 1ml of staining buffer were sequentially added to each well. Following a 30min dyeing process at 4°C, cells were observed under a fluorescent microscope.

Measurement of intracellular ROS

According to the manufacturer's instructions, intracellular ROS were detected using a ROS fluorescence assay kit. As soon as the treatments were completed, serum-free DMEM with 10μM 2,7-dichlorodihydrofluorescein diacetate was replaced for 30 minutes in the dark at 37°C, following that, the cells were washed three times with PBS to remove any residual probe. Under a fluorescence microscope at 10× magnification, images were captured at an excitation wavelength of 488 nm. ImageJ software (Media Cybernetics, Rockville, MD, USA) was used to calculate the mean fluorescence density of fluorescence images.

Lactate Dehydrogenase (LDH) assay

The Cyto Tox 96 Non-Radioactive Cytotoxicity Assay Kit was employed to measure the LDH release. The amount of LDH released was calculated relative to control with maximum lysis (1% Triton X-100 lysed cells).

The Enzyme-Linked Immunosorbent Assay (ELISA)

Based on the manufacturer's guidelines, we measured the concentrations of IL-1β and IL-18 in cell culture supernatants from various treatment and mock groups. In this study, IL-1β and IL-18 Quantikine ELISA Kits were used to detect their levels.

Statistical Analysis

The results were analyzed using the GraphPad Prism 7, and are presented as the mean ± SEM. We evaluated the pairwise differences between the groups using the Student's *t*-test with Welch's correction to determine the statistical significance. In cases where there were more than two groups, we used a one-way analysis of variance (ANOVA). Statistical significance was defined as a P-value of less than 0.05.

Results

Overexpression of canonical pyroptosis-related factors in periodontitis

Gingival tissues were obtained from patients with severe periodontitis and the age-matched healthy subjects. Representative hematoxylin-eosin (HE) staining indicated the presence of a large infiltration of inflammatory cells in the gingival tissue of patients with periodontitis(Fig. 1a). The IHC assay revealed increased expressions of GSDMD in gingival tissues from periodontitis patients (Fig. 1b). Notably, periodontitis tissue sections exhibited strong immunostaining for macrophage marker CD68 in IHC analysis (Fig. 1c). Furthermore, IHC double staining showed GSDMD expression was higher in macrophages expressing the surface marker CD68 (Fig. 1d). To further verify the occurrence of pyroptosis in periodontitis, we measured the expression of pyroptosis-related factors like NF-κB, NLRP3, GSDMD-N, and IL-1β by qRT-PCR, which showed significantly increased expressions of these target genes in periodontitis gingival tissues (Fig. 1e, f, g, h). Altogether, the above results suggest that periodontitis was associated with the occurrence of pyroptosis, and localized macrophages were the major immune cells involved in the process.

Identification and characterization of hPDLSCs

hPDLSCs were isolated using the tissue block method. The primary culture demonstrated a spindle-shaped fibroblast-like morphology (Fig. 2a). After 10–14 days of culture at a low density, single cells could effectively form evenly distributed colonies on the culture dish (Fig. 2b). Flow cytometric analysis revealed positive expression for cell surface markers CD29 (Fig. 2f), CD73 (Fig. 2g), CD90 (Fig. 2h), and CD105 (Fig. 2i), but not CD45 (Fig. 2e). Lipogenic differentiation was induced for 28 days, and lipid droplet formation was visible after oil red O staining (Fig. 2c). For osteogenic differentiation, cells were induced for 26 days, and calcified nodules were then examined by alizarin red S staining (Fig. 2d). Thus, we demonstrated successful isolation and optimized culture condition of patient-derived PDLSCs *in vitro*.

P. gingivalis **-derived LPS triggers canonical pyroptosis in THP-1 cells** in vitro

To determine whether *P.g*-LPS in combination with ATP could effectively induce pyroptosis in THP-1 cells *in vitro*, we first treated THP-1 cells with 0, 0.1, 1, or 10μg/ml of *P.g*-LPS for 11h, followed by 1h exposure to 5mM ATP. The qRT-PCR analysis showed that expressions of NF-κB, NLRP3, caspase-1, GSDMD-N, and IL-1β have significantly increased in a *P.g*-LPS concentration-dependent manner, and the most obvious effect was observed at 10μg/ml of *P.g*-LPS combined with ATP (Fig. 3a). Furthermore, we extracted total

cellular proteins from each of the treated and control groups to determine the protein levels of target genes by western blotting, which were consistent with the qRT-PCR results (Fig. 3b). Fluorescence-microscopically, it was observed that 1μg/ml and 10μg/ml concentrations of *P. gingivalis*-derived LPS combined with ATP could induce substantial changes in cellular membrane integrity at 12h post-exposure. A Hoechst 33324 stain was applied to the nucleus, while PI was applied to dying cells with damaged membranes (Fig. 3c). The CCK8 results showed that the cell survival rate was similar (~ 85%) at both concentrations of *P.g*-LPS (Fig. 3d). Together, these results suggest that sequential treatment with 10μg/ml of *P.g*-LPS for 11h followed by 1h of 5mM ATP can effectively induce the canonical pyroptosis pathway in THP-1 cells.

hPDLSCs prevent THP-1 cells from undergoing the canonical pyroptosis pathway via paracrine secretion

At the mRNA level

As shown before, combined treatment with *P.g*-LPS and ATP can activate the canonical pyroptosis pathway in THP-1 cells following the treatment in the coculture system(Fig. 4a) for 24 h. We found that PDLSCs did not exert any regulatory effects on normal THP-1 cells via the canonical pyroptosis pathway but significantly suppressed expressions of related factors, including NF-κB (Fig. 4b), NLRP3 (Fig. 4c), caspase-1 (Fig. 4d), GSDMD (Fig. 4e), IL-1β (Fig. 4f), and IL-18 (Fig. 4g) in THP-1 cells undergoing pyroptosis. Importantly, following the 24h recovery period of THP-1 cells, the level of pyroptosis was considerably higher in the SCC group compared to that of the SCP group of cells, suggesting that once pyroptosis is induced, it cannot be completely reverted back to the normal condition in 24h even if the inducing factors are removed from the cell environment.

At the protein level

To further confirm the above observations, we measured the protein levels of NF-κB, NLRP3, pro-caspase-1, cleaved-caspase-1, ASC, GSDMD, GSDMD-N, IL-1β, and cleaved-IL-1β by western blotting (Fig. 5a). As expected, the protein expressions were significantly higher in the SCP group, along with the SCC and CCC groups, but were significantly lower in the CCP group than those in the SCP group, which was consistent with the qRT-PCR results. The ELISA were used to detect expressions of IL-1β (Fig. 5b) and IL-18 (Fig. 5c) in the supernatant of each control and treatment groups. The results showed that these indicators were significantly downregulated following the pyroptosis induction in the CCP group but did neither have any functional impact on THP-1 cells under the coculture condition nor produce any cytotoxic effects. Previous studies have confirmed that caspase-1 activation is a pivotal step in initiating the canonical pyroptosis[34–35]. The caspase-1 activity measurement revealed that the combination of *P.g*-LPS and ATP markedly enhanced the caspase-1 activity in THP-1 cells, but coculturing with hPDLSCs significantly reversed the condition (Fig. 5d).

At the cellular level

The integrity of cellular membranes was evaluated by the double staining with Hoechst 33342 and PI. The nuclei were stained with Hoechst 33324, while a higher intracellular intensity of PI signal indicated compromised membrane integrity under the stressed condition (Fig. 6a). As compared to the negative control, exposure to *P.g*-LPS/ATP regimen significantly increased the proportion of PI-permeable cells (red) with damaged membranes. And in the presence of hPDLSCs, the percentage of PI-positive cells was decreased significantly. It has been shown that damaged mitochondria can exacerbate ROS production, which may trigger pyroptosis[36]. Thus, by using 2 ,7 -dichlorodihydrofluorescein diacetate fluorescence probe, we measured ROS levels in THP-1 cells after exposing to *P.g*-LPS and ATP, with or without coculturing with PDLSCs. Figure 6b illustrates that *P.g*-LPS/ATP combination significantly increased the ROS level in THP-1 cells, while hPDLSCs coculture attenuated the ROS-mediated oxidative stress through paracrine secretion. Cytotoxicity Assay kits were used to detect the amount of LDH release (Fig. 6c), we got the result as expected. Cumulatively, these data suggest that the paracrine effect of hPDLSCs can suppress the canonical pyroptosis pathway induction by inhibiting the NF-κB/NLRP3/GSDMD signaling axis in THP-1 macrophages.

Discussion

Periodontitis is an inflammatory disease that causes the loss of periodontal bone and teeth[37]. A growing body of evidence indicates that pyroptosis is a key pathway in the development of periodontitis and associated inflammatory responses[38]. We showed that the key executor of pyroptosis, GSDMD, was highly expressed in the gingival tissue of patients with periodontitis. The pyroptotic macrophages release pro-inflammatory cytokines like IL-1β and IL-18[39]to stimulate the osteoclastogenesis, and bone regeneration processes[40–41]. Besides, upregulation of prostaglandin E2 (PGE2) expression in periodontal ligament cells in response to IL-1β induction increases the production of receptor activator of NF-κB ligand (RANKL) to promote osteoclastogenesis[42], while IL-18 induces several matrix metalloproteases (MMPs) including MMP1, MMP2, MMP3, and MMP9 in periodontal ligament cells, thus potentially increasing the osteoclast resorption capacity[43]. Therefore, pyroptosis is a crucial factor in alveolar bone resorption and may be targeted for periodontal therapy.

Macrophages form the first line of defense against periodontal pathogens and are important components for immune and inflammatory responses[44]. However, when activated macrophages produce excessive inflammatory mediators and proinflammatory cytokines, they initiate a systemic inflammatory process in conjunction with other immune pathways, which could be fatal under certain conditions[45–46]. Our findings also suggest that inflamed periodontal tissues, including the epithelial and lamina propria layers, can be heavily infiltrated with macrophages. Macrophage-associated pyroptosis is a key inducer of several refractory diseases. It is reported that nicotine induces atherosclerosis, which increases the number of TUNEL-positive macrophages as well as caspase1 expression, in addition to increased serum levels of IL-1β and IL-18[47].Wu et al. have shown that caspase-1 is activated in LPS-induced acute lung

injury to facilitate the alveolar macrophage pyroptosis, which can serve as a potential therapeutic target[48], coincidentally, Li et al. considered that inhibition of macrophage pyroptosis may provide a novel immunotherapy strategy for acute lung injury[49]. Notably, there are only a few reports on the role of macrophage pyroptosis in the pathogenesis of periodontitis. Therefore, we were the first to report that $CD68^+$ macrophages were the main pyroptosis initiator in periodontal inflammatory tissues and play a key role in the development of periodontitis.

To further understand the molecular mechanism of macrophage-related pyroptosis in periodontitis, we investigated the underlying signaling pathways. There are multiple caspases that mediate cellular pyroptosis, such as caspase-1, 4, 5, 11 (4, & 5 are found in humans)[50]. By interacting with pro-caspase-1, NLRP3 participates in the formation of NLRP3 inflammasome through the canonical pyroptosis pathway[51], whereas caspases-4/5 (in humans) and caspase-11 (in mice) modulate the non-canonical signaling pathway[52–53]. The activated caspase-1 catalyzes the conversion of pro-IL-1β and pro-IL-18 into their mature forms, IL-1β and IL-18[34], while caspase-4/5/11 exhibit a mild ability to process pro-IL-1β and pro-IL-18[35]. Caspase-4/5/11 mainly induce pyroptosis through caspase-1 activation, suggesting that caspase-1 activation is essential for pyroptosis.

Therefore, we mainly examined the pyroptosis pathway in macrophages through the NF-κb/NLRP3/GSDMD signaling pathway. NLRP3 is shown to bind pro-caspase-1 through ASC to constitute the NLRP3 inflammasome and subsequent activating caspase-1. This mechanism requires two signals to activate the whole cascade. First, NF-κB gets activated upon pathogenic and/or inflammatory responses (e.g., LPS exposure), and binds Toll-like receptor 4 (TLR4) to induce the expression of NLRP3, caspase-1, pro-IL-1β, and pro-IL-18. Moreover, extracellular ATP or bacterial toxins can directly cause the activation of caspass-1, leading to the secretion of IL-1β and IL-18[54]. It has been found that elevated ATP levels can also trigger excessive ROS production[55]. Additionally, GSDMD-mediated pyroptosis has been linked to increased ROS generation in macrophages[36]. Indeed, *Escherichia coli* LPS-primed macrophages can be treated with ATP to induce pyroptosis[56]. In an attempt to mimic the pathogenetic process of periodontitis, we induced macrophages with *P. gingivalis* LPS combined with ATP, and observed that it could induce the characteristic pyroptotic morphology, stimulate the cleavage of GSDMD-N terminal domain, and activate IL-1β and caspase-1.

The use of PDLSCs is currently being proposed and explored in periodontal regeneration. A number of studies have demonstrated that PDLSCs are capable of self-differentiation and can be used directly to restore alveolar bone damage[57–59]. A recent study has investigated the immunomodulatory role of PDLSCs[60]. But, there is a poor understanding about the immunomodulatory mechanism of PDLSCs. Therefore, after successfully inducing macrophage pyroptosis, we performed *in vitro* coculture of PDLSCs with pyroptotic cells. We found that the gene expression and protein levels of associated factors like NF-κB, NLRP3, caspase-1, ASC, GSDMD, IL-1β, and IL-18, were significantly lower in the coculture group compared with the pyroptosis alone group. Furthermore, we validated the inhibitory effects of PDLSCs on pyroptosis of macrophages by measuring the caspase-1 activity, ROS levels, and membrane integrity by

dual staining with Hoechst 33342/PI. Taken together, these findings suggest that PDLSCs can inhibit the occurrence of pyroptosis through paracrine effects via the NF-κB/NLRP3/GSDMD signaling axis, but the specific sites of action need to be further explored.

Conclusion

In this study, we found that macrophage pyroptosis was essential in the development of periodontitis. The *P. gingivalis*-derived LPS combined with ATP could effectively trigger GSDMD-mediated pyroptosis in THP-1 macrophages *in vitro*. The investigation of the mechanism of action revealed that the paracrine effect of PDLSCs inhibited the NF-κB/NLRP3/GSDMD-mediated activation of the canonical pyroptosis pathway (Fig. 7). The findings of this study might provide us with new therapeutic targets for the treatment of periodontitis and further highlight the immunomodulatory roles of PDLSCs in periodontal disease management.

Abbreviations

P-gingivalis
Porphyromonas gingivalis
LPS
lipopolysaccharide
P.g-LPS
Porphyromonas gingivalis-derived lipopolysaccharide
ATP
adenosine triphosphate
PDLSCs
periodontal ligament stem cells
hPDLSCs
human periodontal ligament-derived stem cells
NLRP3
NOD-like receptor family pyrin domain-containing protein 3
ASC
apoptosis-associated speck-like protein containing a CARD
GSDMD
gasdermin-D
IL-1β/18
interleukin-1β/18
GAPDH
glyceraldehyde 3-phosphate Dehydrogenase
PI
propidium iodide

LDH
lactate dehydrogenase
PAMPs
pathogen-associated molecular patterns
DAMPs
damage-associated molecular patterns
ROS
reactive oxygen species
PMA
phorbol myristate acetate
PFA
paraformaldehyde
PS
Penicillin-Streptomycin
DMEM
Dulbecco's modified Eagle medium
PBS
phosphate-buffered saline
FBS
fetal bovine serum
CCK-8
Cell Counting Kit-8
SCC
single-culture control group
SCP
single-culture pyroptosis group
CCC
coculture control group
CCP
coculture pyroptosis group. qRT-PCR:quantitative real-time polymerase chain reaction
ELISA
Enzyme-Linked Immunosorbent Assay
IHC
immunohistochemical
HE
hematoxylin-eosin staining.

Declarations

Ethics approval and consent to participate

This study was approved by the Research Ethics Committee of the Affiliated Hospital of Qingdao University (QYFY WZLL 27126).

Consent for publication

Not applicable.

Availability of data and materials

The datasets supporting the conclusions of this article are included within the article.

Competing interests

The authors declare that they have no competing interests.

Funding

This work was primarily supported by the Natural Science Foundation of Shandong Province, China (Grant No. ZR2019MH003), and the Science and Technology Planning Project of Qingdao (Grant No. 19-6-1-36-nsh).

Authors' contributions

Wenxuan Wang: Investigation, Visualization, Conceptualization, Methodology, Writing original draft. Xu Qiu: Data curation, Investigation. Yingzhe Hu: Visualization, Investigation. Shuhan Li: Investigation. Xiangru Gao: Investigation. Qiuxia Ji: Resources, Supervision, Writing – review & editing.

Acknowledgements

The authors thank the funders listed in the “Funding” section for their support.

Author information

[1] Department of Periodontology, The Affiliated Hospital of Qingdao University, Qingdao 266000, China.
[2] School of Stomatology of Qingdao University, Qingdao 266003, China.

References

1. Hajishengallis G. Periodontitis: from microbial immune subversion to systemic inflammation. Nat Rev Immunol. 2015 Jan;15(1):30–44.
2. Taylor JJ, Jaedicke KM, van de Merwe RC, Bissett SM, Landsdowne N, Whall KM, Pickering K, Thornton V, Lawson V, Yatsuda H, Kogai T, Shah D, Athey D, Preshaw PM. A Prototype Antibody-based Biosensor for Measurement of Salivary MMP-8 in Periodontitis using Surface Acoustic Wave Technology. Sci Rep. 2019 Jul;30(1):11034. 9(.

3. US Preventive Services Task Force. Davidson KW, Barry MJ, Mangione CM, Cabana M, Chelmow D, Coker TR, Davis EM, Donahue KE, Jaén CR, Krist AH, Kubik M, Li L, Ogedegbe G, Pbert L, Ruiz JM, Stevermer J, Tseng CW, Wong JB. Aspirin Use to Prevent Cardiovascular Disease: US Preventive Services Task Force Recommendation Statement. JAMA. 2022 Apr 26;327(16):1577–84.
4. Yun LW, Decarlo AA, Hunter N. Blockade of protease-activated receptors on T cells correlates with altered proteolysis of CD27 by gingipains of Porphyromonas gingivalis. Clin Exp Immunol. 2007 Nov;150(2):217–29.
5. Ao M, Miyauchi M, Inubushi T, Kitagawa M, Furusho H, Ando T, Ayuningtyas NF, Nagasaki A, Ishihara K, Tahara H, Kozai K, Takata T. Infection with Porphyromonas gingivalis exacerbates endothelial injury in obese mice. PLoS One. 2014 Oct 21;9(10):e110519.
6. Sawa Y, Takata S, Hatakeyama Y, Ishikawa H, Tsuruga E. Expression of toll-like receptor 2 in glomerular endothelial cells and promotion of diabetic nephropathy by Porphyromonas gingivalis lipopolysaccharide. PLoS One. 2014 May 16;9(5):e97165.
7. Bender P, Bürgin WB, Sculean A, Eick S. Serum antibody levels against Porphyromonas gingivalis in patients with and without rheumatoid arthritis - a systematic review and meta-analysis. Clin Oral Investig. 2017 Jan;21(1):33–42. Epub 2016 Aug 25.
8. He WT, Wan H, Hu L, Chen P, Wang X, Huang Z, Yang ZH, Zhong CQ, Han J. Gasdermin D is an executor of pyroptosis and required for interleukin-1β secretion. Cell Res. 2015 Dec;25(12):1285–98. doi: 10.1038/cr.2015.139 Epub 2015 Nov 27.
9. Feng S, Fox D, Man SM. Mechanisms of Gasdermin Family Members in Inflammasome Signaling and Cell Death. J Mol Biol. 2018 Sep 14;430(18 Pt B):3068–3080 Epub 2018 Jul 7.
10. Xia S, Zhang Z, Magupalli VG, Pablo JL, Dong Y, Vora SM, Wang L, Fu TM, Jacobson MP, Greka A, Lieberman J, Ruan J, Wu H. Gasdermin D pore structure reveals preferential release of mature interleukin-1. Nature. 2021 May;593(7860):607–11. Epub 2021 Apr 21.
11. Hu Z, Murakami T, Suzuki K, Tamura H, Kuwahara-Arai K, Iba T, Nagaoka I. Antimicrobial cathelicidin peptide LL-37 inhibits the LPS/ATP-induced pyroptosis of macrophages by dual mechanism. PLoS One. 2014 Jan 16;9(1):e85765.
12. Tonnus W, Linkermann A. The in vivo evidence for regulated necrosis. Immunol Rev. 2017 May;277(1):128–149.
13. Kayagaki N, Stowe IB, Lee BL, O'Rourke K, Anderson K, Warming S, Cuellar T, Haley B, Roose-Girma M, Phung QT, Liu PS, Lill JR, Li H, Wu J, Kummerfeld S, Zhang J, Lee WP, Snipas SJ, Salvesen GS, Morris LX, Fitzgerald L, Zhang Y, Bertram EM, Goodnow CC, Dixit VM. Caspase-11 cleaves gasdermin D for non-canonical inflammasome signalling. Nature. 2015 Oct 29;526(7575):666 – 71 Epub 2015 Sep 16.
14. Gao L, Dong X, Gong W, Huang W, Xue J, Zhu Q, Ma N, Chen W, Fu X, Gao X, Lin Z, Ding Y, Shi J, Tong Z, Liu T, Mukherjee R, Sutton R, Lu G, Li W. Acinar cell NLRP3 inflammasome and gasdermin D (GSDMD) activation mediates pyroptosis and systemic inflammation in acute pancreatitis. Br J Pharmacol. 2021 Sep;178(17):3533–52. Epub 2021 May 21.

15. Yamaguchi Y, Kurita-Ochiai T, Kobayashi R, Suzuki T, Ando T. Regulation of the NLRP3 inflammasome in Porphyromonas gingivalis-accelerated periodontal disease. Inflamm Res. 2017 Jan;66(1):59–65 Epub 2016 Sep 24.
16. García-Hernández AL, Muñoz-Saavedra ÁE, González-Alva P, Moreno-Fierros L, Llamosas-Hernández FE, Cifuentes-Mendiola SE, Rubio-Infante N. Upregulation of proteins of the NLRP3 inflammasome in patients with periodontitis and uncontrolled type 2 diabetes. Oral Dis. 2019 Mar;25(2):596–608. Epub 2018 Dec 16.
17. Ma C, Yang D, Wang B, Wu C, Wu Y, Li S, Liu X, Lassen K, Dai L, Yang S. Gasdermin D in macrophages restrains colitis by controlling cGAS-mediated inflammation. Sci Adv. 2020 May;20(21):eaaz6717. 6(.
18. dos Santos G, Rogel MR, Baker MA, Troken JR, Urich D, Morales-Nebreda L, Sennello JA, Kutuzov MA, Sitikov A, Davis JM, Lam AP, Cheresh P, Kamp D, Shumaker DK, Budinger GR, Ridge KM. Vimentin regulates activation of the NLRP3 inflammasome. Nat Commun. 2015 Mar 12;6:6574.
19. Jo EK, Kim JK, Shin DM, et al. Molecular mechanisms regulating NLRP3 inflammasome activation. Cell Mol Immunol. 2016 Mar;13(2):148–59 Epub 2015 Nov 9.
20. Gutiérrez-Venegas G, Maldonado-Frías S, Ontiveros-Granados A, et al. Role of p38 in nitric oxide synthase and cyclooxygenase expression, and nitric oxide and PGE2 synthesis in human gingival fibroblasts stimulated with lipopolysaccharides. Life Sci. 2005 May;20(1):60–73. 77(.
21. Hosokawa Y, Hosokawa I, Ozaki K, et al. CXCL12 and CXCR4 expression by human gingival fibroblasts in periodontal disease. Clin Exp Immunol. 2005 Sep;141(3):467–74.
22. Khan MS, Ikram M, Park JS, et al, Its Role in Induction of Alzheimer's Disease Pathology, and Possible Therapeutic Interventions: Special Focus on Anthocyanins. Cells. 2020 Apr 1;9(4):853.
23. Song W, Wei L, Du Y, Wang Y, Jiang S. Protective effect of ginsenoside metabolite compound K against diabetic nephropathy by inhibiting NLRP3 inflammasome activation and NF-κB/p38 signaling pathway in high-fat diet/streptozotocin-induced diabetic mice. Int Immunopharmacol. 2018 Oct;63:227–38. Epub 2018 Aug 11.
24. Cai SM, Yang RQ, Li Y, Ning ZW, Zhang LL, Zhou GS, Luo W, Li DH, Chen Y, Pan MX, Li X. Angiotensin-(1–7) Improves Liver Fibrosis by Regulating the NLRP3 Inflammasome via Redox Balance Modulation. Antioxid Redox Signal. 2016 May 10;24(14):795–812 Epub 2016 Mar 22.
25. Jansen JE, Gaffney EA, Wagg J, Coles MC. Combining Mathematical Models With Experimentation to Drive Novel Mechanistic Insights Into Macrophage Function. Front Immunol. 2019 Jun;6:10:1283.
26. Goldszmid RS, Trinchieri G. The price of immunity. Nat Immunol. 2012 Oct;13(10):932–8. Epub 2012 Sep 18.
27. Guzik TJ, Korbut R, Adamek-Guzik T. Nitric oxide and superoxide in inflammation and immune regulation. J Physiol Pharmacol. 2003 Dec;54(4):469–87.
28. Nathan C. Points of control in inflammation. Nature. 2002 Dec 19–26;420(6917):846–52.
29. Chen FM, Sun HH, Lu H, Yu Q. Stem cell-delivery therapeutics for periodontal tissue regeneration. Biomaterials. 2012 Sep;33(27):6320–44. Epub 2012 Jun 12.

30. Park JY, Jeon SH, Choung PH. Efficacy of periodontal stem cell transplantation in the treatment of advanced periodontitis. Cell Transpl. 2011;20(2):271–85. Epub 2010 Aug 18.
31. Ou Q, Miao Y, Yang F, Lin X, Zhang LM, Wang Y.. Zein/gelatin/nanohydroxyapatite nanofibrous scaffolds are biocompatible and promote osteogenic differentiation of human periodontal ligament stem cells. Biomater Sci. 2019 Apr 23;7(5):1973–1983.
32. Zheng Y, Dong C, Yang J, Jin Y, Zheng W, Zhou Q, Liang Y, Bao L, Feng G, Ji J, Feng X, Gu Z. Exosomal microRNA-155-5p from PDLSCs regulated Th17/Treg balance by targeting sirtuin-1 in chronic periodontitis. J Cell Physiol. 2019 Nov;234(11):20662–74. Epub 2019 Apr 23.
33. Pan C, Liu J, Wang H, Song J, Tan L, Zhao H. Porphyromonas gingivalis can invade periodontal ligament stem cells. BMC Microbiol. 2017 Feb 17;17(1):38.
34. van de Veerdonk FL, Netea MG, Dinarello CA, Joosten LA. Inflammasome activation and IL-1β and IL-18 processing during infection. Trends Immunol. 2011 Mar;32(3):110–6 Epub 2011 Feb 18.
35. Downs KP, Nguyen H, Dorfleutner A, Stehlik C. An overview of the non-canonical inflammasome. Mol Aspects Med. 2020 Dec;76:100924 Epub 2020 Nov 11.
36. Wang Y, Shi P, Chen Q, Huang Z, Zou D, Zhang J, Gao X, Lin Z. Mitochondrial ROS promote macrophage pyroptosis by inducing GSDMD oxidation. J Mol Cell Biol. 2019 Dec 19;11(12):1069–1082.
37. Van Dyke TE. Pro-resolving mediators in the regulation of periodontal disease. Mol Aspects Med. 2017 Dec;58:21–36. Epub 2017 May 18.
38. Sordi MB, Magini RS, Panahipour L, Gruber R. Pyroptosis-Mediated Periodontal Disease. Int J Mol Sci. 2021 Dec 29;23(1):372.
39. Kesavardhana S, Malireddi RKS, Kanneganti TD. Caspases in Cell Death, Inflammation, and Pyroptosis. Annu Rev Immunol. 2020 Apr 26;38:567–595 Epub 2020 Feb 4.
40. Evavold CL, Kagan JC. How Inflammasomes Inform Adaptive Immunity. J Mol Biol. 2018 Jan 19;430(2):217–237 Epub 2017 Oct 5.
41. Auréal M, Machuca-Gayet I, Coury F. Rheumatoid Arthritis in the View of Osteoimmunology. Biomolecules. 2020 Dec 31;11(1):48.
42. Murayama R, Kobayashi M, Takeshita A, Yasui T, Yamamoto M. MAPKs, activator protein-1 and nuclear factor-κB mediate production of interleukin-1β-stimulated cytokines, prostaglandin E_2 and MMP-1 in human periodontal ligament cells. J Periodontal Res. 2011 Oct;46(5):568–75 Epub 2011 May 25.
43. Wang F, Guan M, Wei L, Yan H. IL–18 promotes the secretion of matrix metalloproteinases in human periodontal ligament fibroblasts by activating NF–κB signaling. Mol Med Rep. 2019 Jan;19(1):703–10. Epub 2018 Nov 26.
44. Posadas I, De Rosa S, Terencio MC, Payá M, Alcaraz MJ. Cacospongionolide B suppresses the expression of inflammatory enzymes and tumour necrosis factor-alpha by inhibiting nuclear factor-kappa B activation. Br J Pharmacol. 2003 Apr;138(8):1571–9.

45. Zhang G, Ghosh S. Molecular mechanisms of NF-kappaB activation induced by bacterial lipopolysaccharide through Toll-like receptors. J Endotoxin Res. 2000;6(6):453–7.
46. Libby P. Inflammation and cardiovascular disease mechanisms. Am J Clin Nutr. 2006 Feb;83(2):456S–460S.
47. Xu S, Chen H, Ni H, Dai Q. Targeting HDAC6 attenuates nicotine-induced macrophage pyroptosis via NF-κB/NLRP3 pathway. Atherosclerosis. 2021 Jan;317:1–9. Epub 2020 Nov 24.
48. Wu DD, Pan PH, Liu B, Su XL, Zhang LM, Tan HY, Cao Z, Zhou ZR, Li HT, Li HS, Huang L, Li YY. Inhibition of Alveolar Macrophage Pyroptosis Reduces Lipopolysaccharide-induced Acute Lung Injury in Mice. Chin Med J (Engl). 2015 Oct 5;128(19):2638-45.
49. Li D, Ren W, Jiang Z, Zhu L. Regulation of the NLRP3 inflammasome and macrophage pyroptosis by the p38 MAPK signaling pathway in a mouse model of acute lung injury. Mol Med Rep. 2018 Nov;18(5):4399–409. Epub 2018 Aug 24.
50. Shi J, Zhao Y, Wang K, Shi X, Wang Y, Huang H, Zhuang Y, Cai T, Wang F, Shao F. Cleavage of GSDMD by inflammatory caspases determines pyroptotic cell death. Nature. 2015 Oct 29;526(7575):660–5 Epub 2015 Sep 16.
51. Wang Y, Chen Q, Jiao F, Shi C, Pei M, Wang L, Gong Z. Histone deacetylase 2 regulates ULK1 mediated pyroptosis during acute liver failure by the K68 acetylation site. Cell Death Dis. 2021 Jan 11;12(1):55.
52. Yang J, Zhao Y, Shao F. Non-canonical activation of inflammatory caspases by cytosolic LPS in innate immunity. Curr Opin Immunol. 2015 Feb;32:78–83. Epub 2015 Jan 24.
53. Baker PJ, Boucher D, Bierschenk D, Tebartz C, Whitney PG, D'Silva DB, Tanzer MC, Monteleone M, Robertson AA, Cooper MA, Alvarez-Diaz S, Herold MJ, Bedoui S, Schroder K, Masters SL. NLRP3 inflammasome activation downstream of cytoplasmic LPS recognition by both caspase-4 and caspase-5. Eur J Immunol. 2015 Oct;45(10):2918–26. Epub 2015 Aug 24.
54. Gross O, Thomas CJ, Guarda G, Tschopp J. The inflammasome: an integrated view. Immunol Rev. 2011 Sep;243(1):136–51.
55. Sun Y, Jin C, Zhang X, Jia W, Le J, Ye J. Restoration of GLP-1 secretion by Berberine is associated with protection of colon enterocytes from mitochondrial overheating in diet-induced obese mice. Nutr Diabetes. 2018 Sep;24(1):53. 8(.
56. Liang YD, Bai WJ, Li CG, Xu LH, Wei HX, Pan H, He XH, Ouyang DY. Piperine Suppresses Pyroptosis and Interleukin-1β Release upon ATP Triggering and Bacterial Infection. Front Pharmacol. 2016 Oct 20;7:390.
57. Liu J, Chen B, Bao J, Zhang Y, Lei L, Yan F. Macrophage polarization in periodontal ligament stem cells enhanced periodontal regeneration. Stem Cell Res Ther. 2019;10(1):320. Published 2019 Nov 15.
58. Vandana KL, Desai R, Dalvi PJ. Autologous Stem Cell Application in Periodontal Regeneration Technique (SAI-PRT) Using PDLSCs Directly From an Extracted Tooth···An Insight. Int J Stem Cells. 2015 Nov;8(2):235–7.

59. Tassi SA, Sergio NZ, Misawa MYO, Villar CC. Efficacy of stem cells on periodontal regeneration: Systematic review of pre-clinical studies. J Periodontal Res. 2017 Oct;52(5):793–812 Epub 2017 Apr 10.
60. Cianci E, Recchiuti A, Trubiani O, Diomede F, Marchisio M, Miscia S, Colas RA, Dalli J, Serhan CN, Romano M. Human Periodontal Stem Cells Release Specialized Proresolving Mediators and Carry Immunomodulatory and Prohealing Properties Regulated by Lipoxins. Stem Cells Transl Med. 2016 Jan;5(1):20–32. Epub 2015 Nov 25.

Tables

Table 1

Sequence of primers used for quantitative polymerase chain reaction assays

Gene		Primer Sequence (5’-3’)
NF-κB	FORWARD:	ATGGTGGTCGGCTTCGCAAAC
	REVERSE:	CGCCTCTGTCATTCGTGCTTCC
NLRP3	FORWARD:	TGGCTGTAACATTCGGAGATTGTGG
	REVERSE:	GCTTCTGGTTGCTGCTGAGGAC
Caspase-1	FORWARD:	GGTGCTGAACAAGGAAGAGATGGAG
	REVERSE:	TGCCTGAGGAGCTGCTGAGAG
GSDMD	FORWARD:	GCCTCCACAACTTCCTGACAGATG
	REVERSE:	GGTCTCCACCTCTGCCCGTAG
GSDMD-N	FORWARD:	GAGCTTCCACTTCTACGATGCCATG
	REVERSE:	CCTGCGATCTTTGCCTGTCCTG
IL-1β	FORWARD:	CAGTGGCAATGAGGATGA
	REVERSE:	TAGTGGTGGTCGGAGATT
IL-18	FORWARD:	TTGACCAAGGAAATCGGCCTC
	REVERSE:	GCCATACCTCTAGGCTGGCT
GAPDH	FORWARD:	TGAAGGTCGGAGTCAACGGATTTGGT
	REVERSE:	CATGTGGGCCATGAGGTCCACCAC

Figures

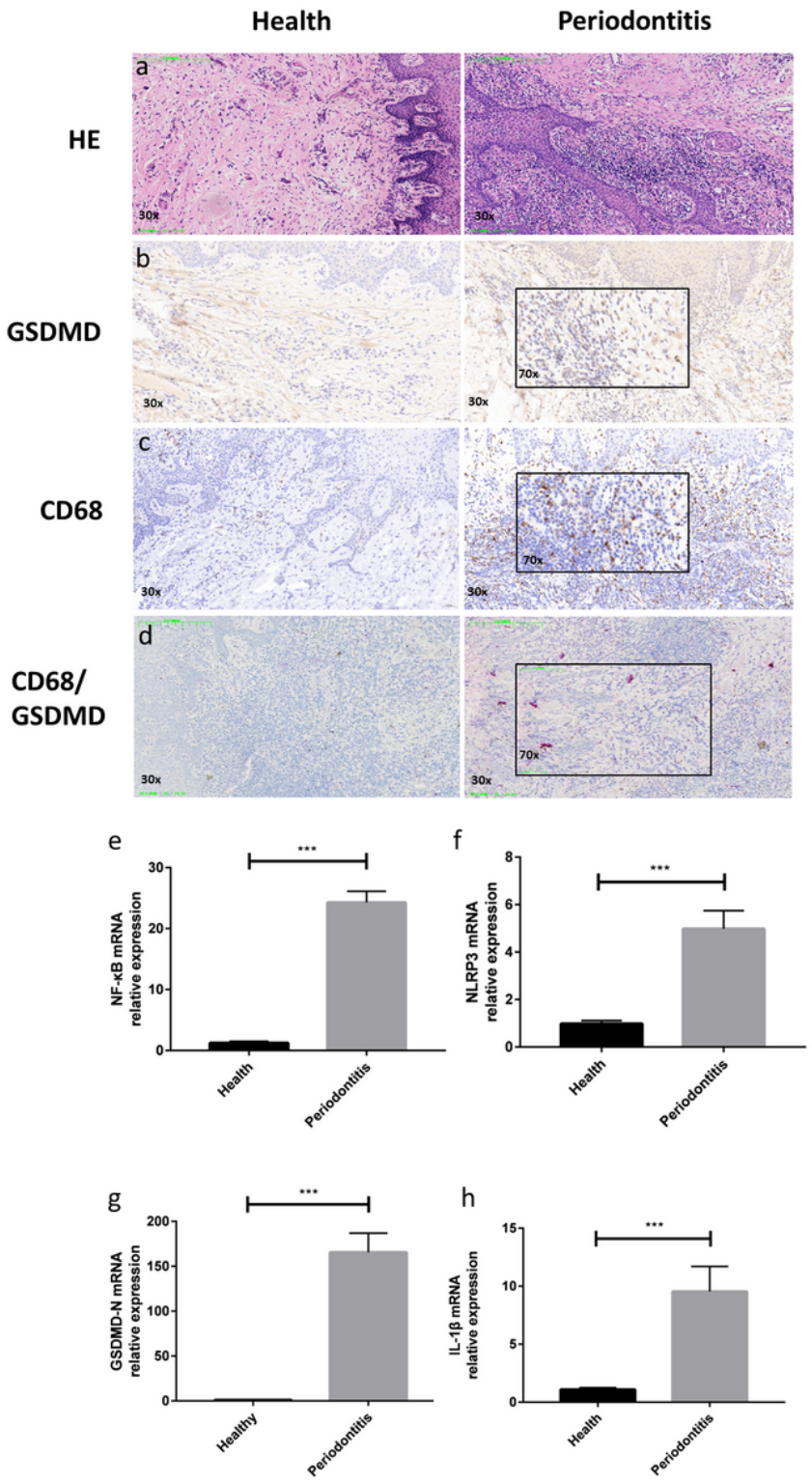

Figure 1

Representative hematoxylin-eosin (HE) staining(a) and immunohistochemical staining of GSDMD(b) and CD68(c) in human gingival tissues sections from healthy and periodontitis patients, the signals of GSDMD and CD68 appear brown in sections counterstained with hematoxylin (blue). For GSDMD/CD68 double immunohistochemical staining(d), GSDMD and CD68 show red and brown respectively. Experiments were repeated independently more than three times. The mRNA levels of NF-κB (e), NLRP3

(f), GSDMD-N (g), and IL-1β (h) were measured by qRT-PCR and normalized to the expression of the housekeeping gene GAPDH. The mRNA levels of cytokines in untreated controls were set to 1.0. Bars show the levels of cytokines as the mean ± SD (n = 3) analyzed by the Student s t-test (*p < 0.05, **p < 0.01, ***p < 0.001).

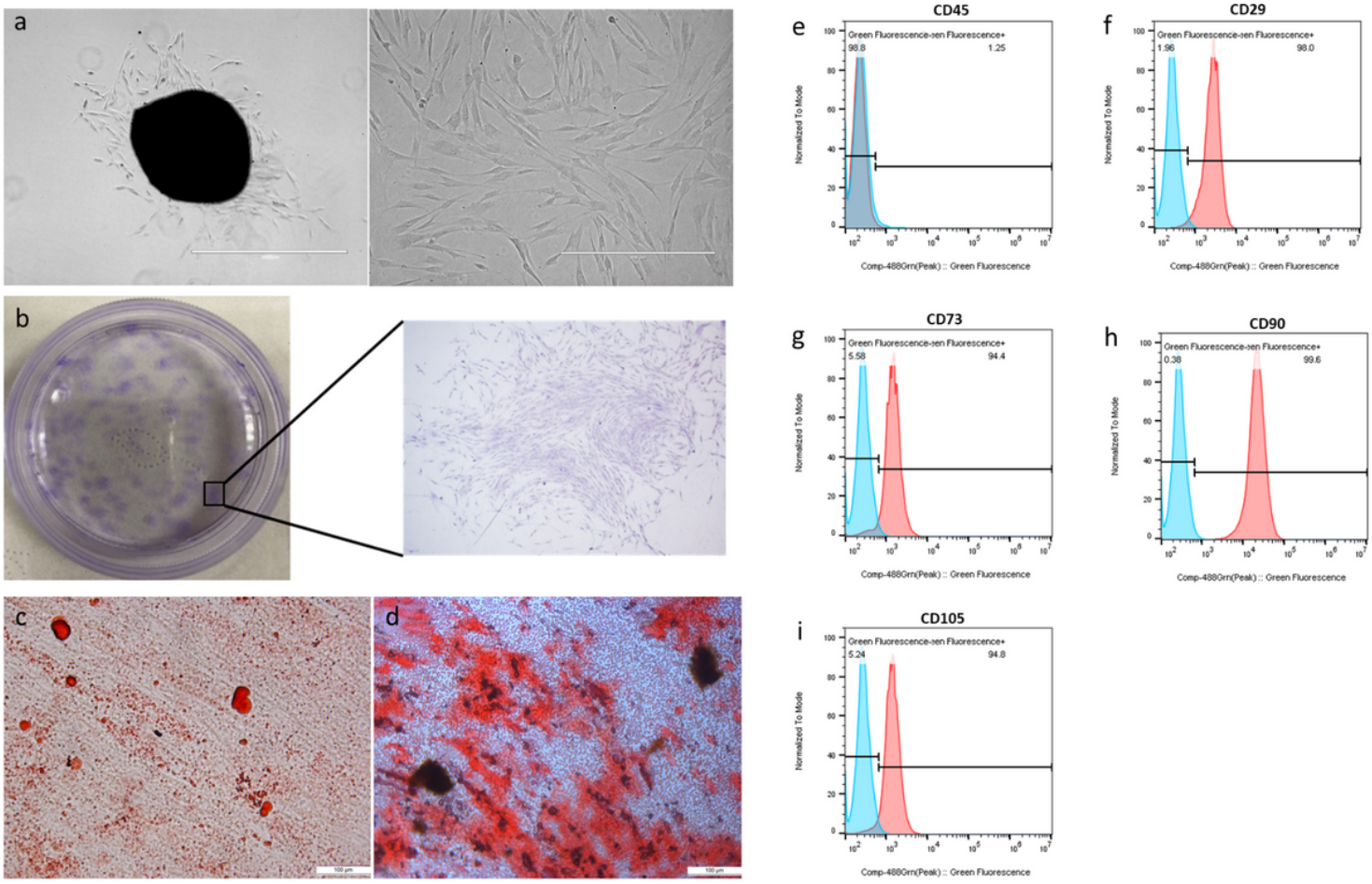

Figure 2

(a) Cultured primary cells derived from human periodontal ligament exhibited typical fibroblast-like morphology; (b) hPDLSCs were plated at low density and stained with 0.1% toluidine blue after 2 weeks; (c) Oil Red O staining of the adipogenically stimulated hPDLSCs; (d) Alizarin Red staining of the osteogenically stimulated hPDLSCs; Flow cytometry analyses of the expression of surface markers CD45(e), CD29(f), CD73(g), CD90(h), CD105(i).

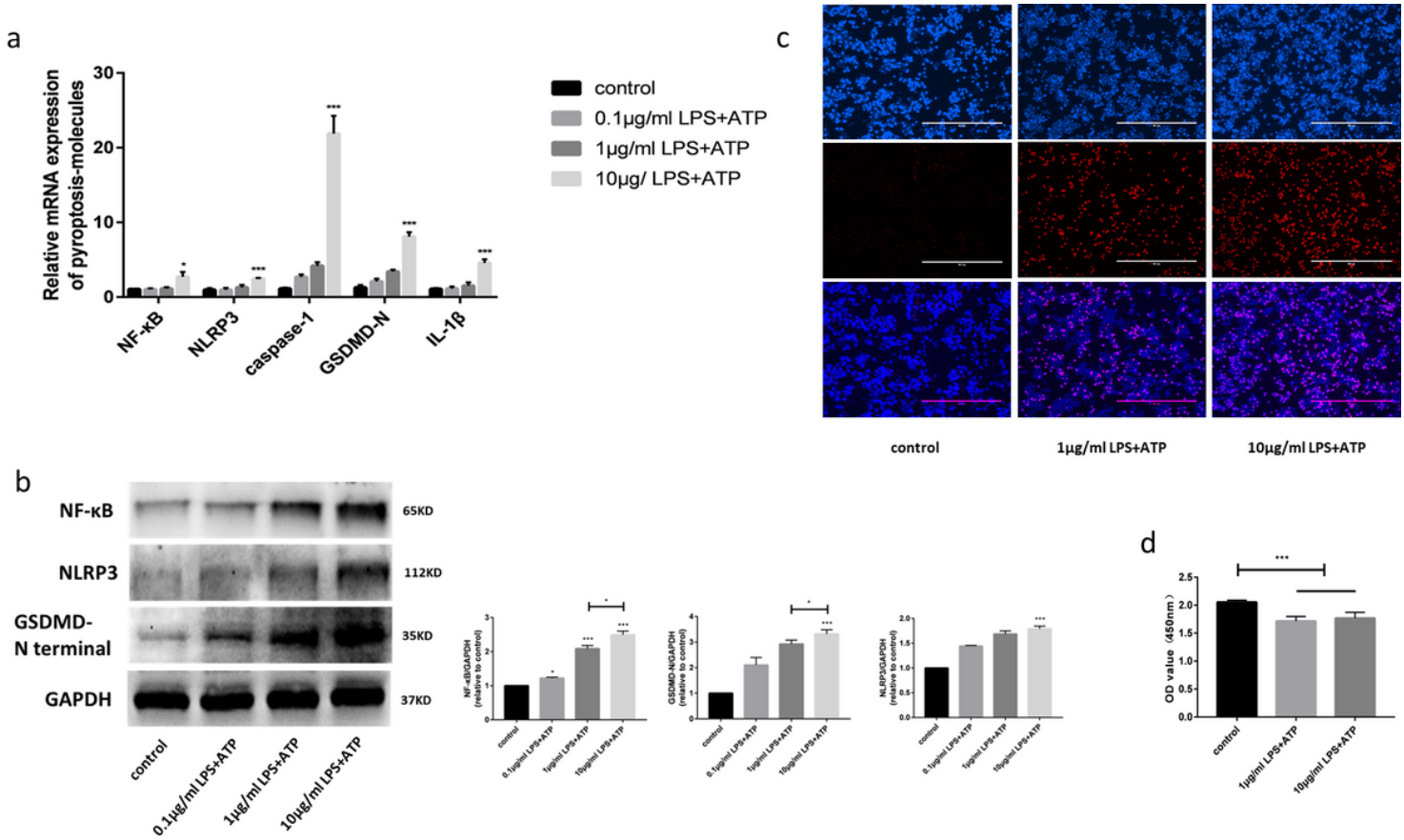

Figure 3

The mRNA levels(a) of NF-κB, NLRP3, caspase-1, GSDMD-N, IL-1β and the protein levels(b) of NF-κB, NLRP3, GSDMD-N in THP-1 macrophages were measured by qRT-PCR and western blotting and normalized to the expression of the GAPDH after 12 hours of being induced at different LPS (*P. gingivalis*) concentrations. The mRNA and protein levels of cytokines in untreated controls were set to 1.0. Bars show the levels of cytokines as the mean ± SD (n = 3) analyzed by the Student s t-test (*p < 0.05, **p < 0.01, ***p < 0.001). Hoechst 33342 and PI double staining images were captured by fluorescence microscopy (×10) (c) and the survival state was measured by cck8 (d) after induction of pyroptosis at different LPS (*P. gingivalis*) concentrations.

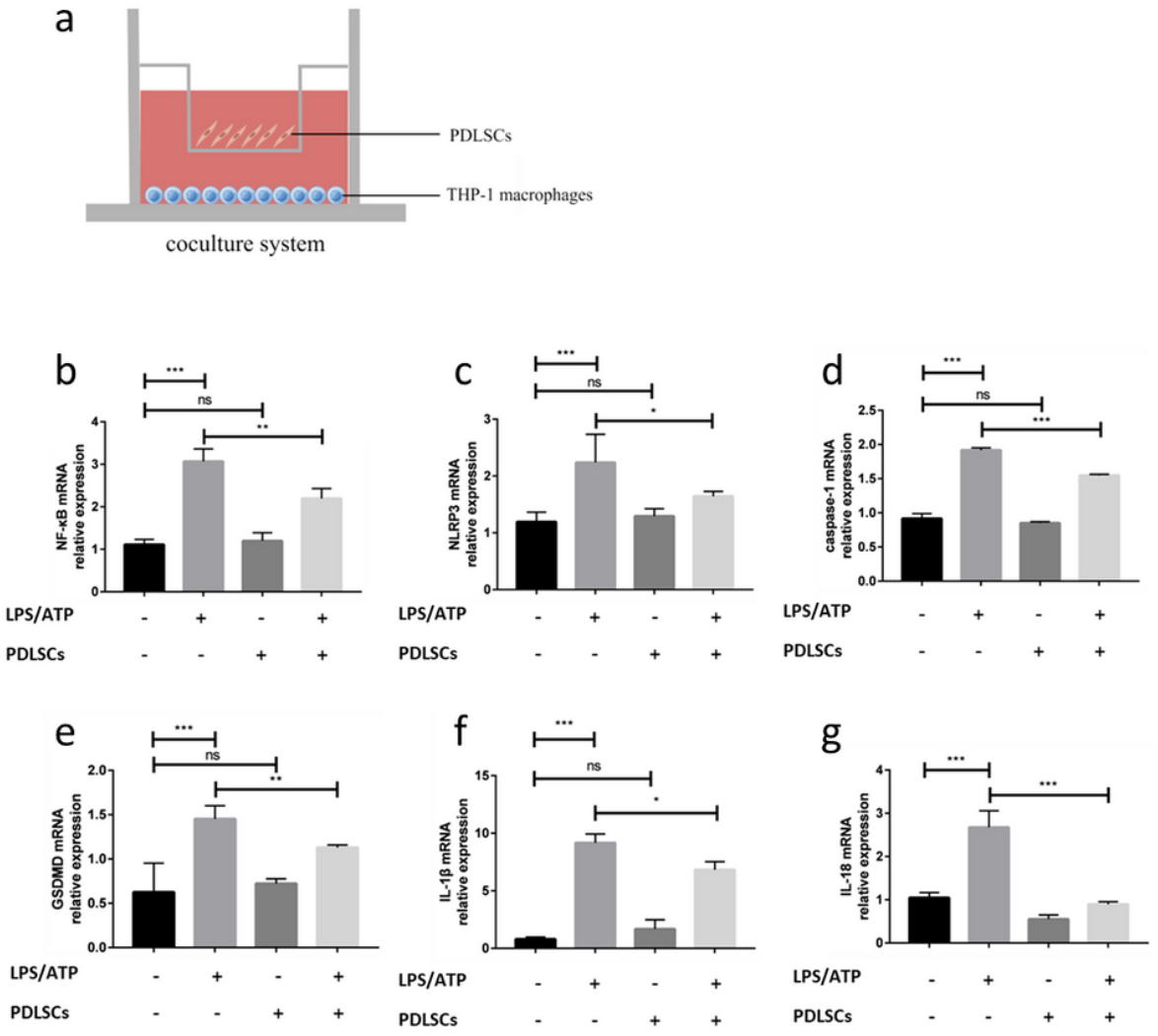

Figure 4

The cells were stimulated with 10μg/ml LPS (*P. gingivalis*) for 11 h, followed 1 h of treatment with 5 mM ATP and then by coculture with PDLSCs for 24 h(a). The mRNA levels of NF-κB1(b), NLRP3(c), caspase-1(d), GSDMD(e), IL-1β(f) and IL-18(g) were measured by qRT-PCR and normalized to the expression of the housekeeping gene GAPDH. The mRNA levels of cytokines in untreated controls were set to 1.0. Bars show the levels of cytokines as the mean ± SD (n = 3) analyzed by the Student s t-test (*p < 0.05, **p < 0.01, ***p < 0.001).

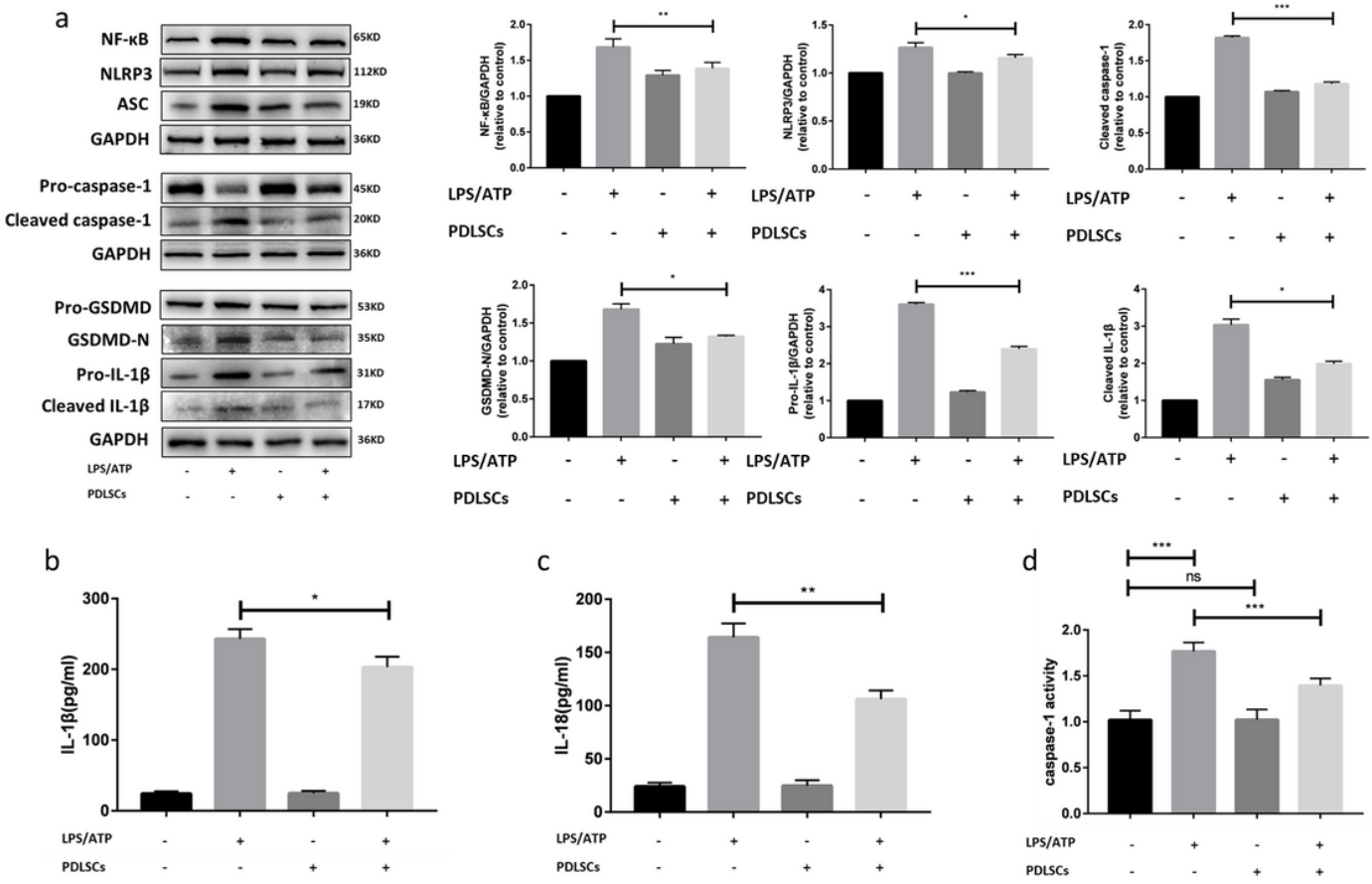

Figure 5

The cells were stimulated with 10μg/ml LPS (*P. gingivalis*) for 11 h, followed 1 h of treatment with 5 mM ATP and then by coculture with PDLSCs for 24 h. (a) Protein levels of NF-κB, NLRP3, ASC, pro-caspase-1, cleaved caspase-1, pro-GSDMD, GSDMD-N, pro-IL-1β, and cleaved IL-1β were measured by western blotting analysis. The blots were stripped and reprobed for GAPDH as a loading control. IL-1β(b) and IL-18(c) in culture medium were measured by ELISA. (d)Activated caspase-1 was measured by a Caspase-1 Activity Assay Kit.Values are the means ± standard deviation (SD) of three independent experiments (*p < 0.05, **p < 0.01, ***p < 0.001).

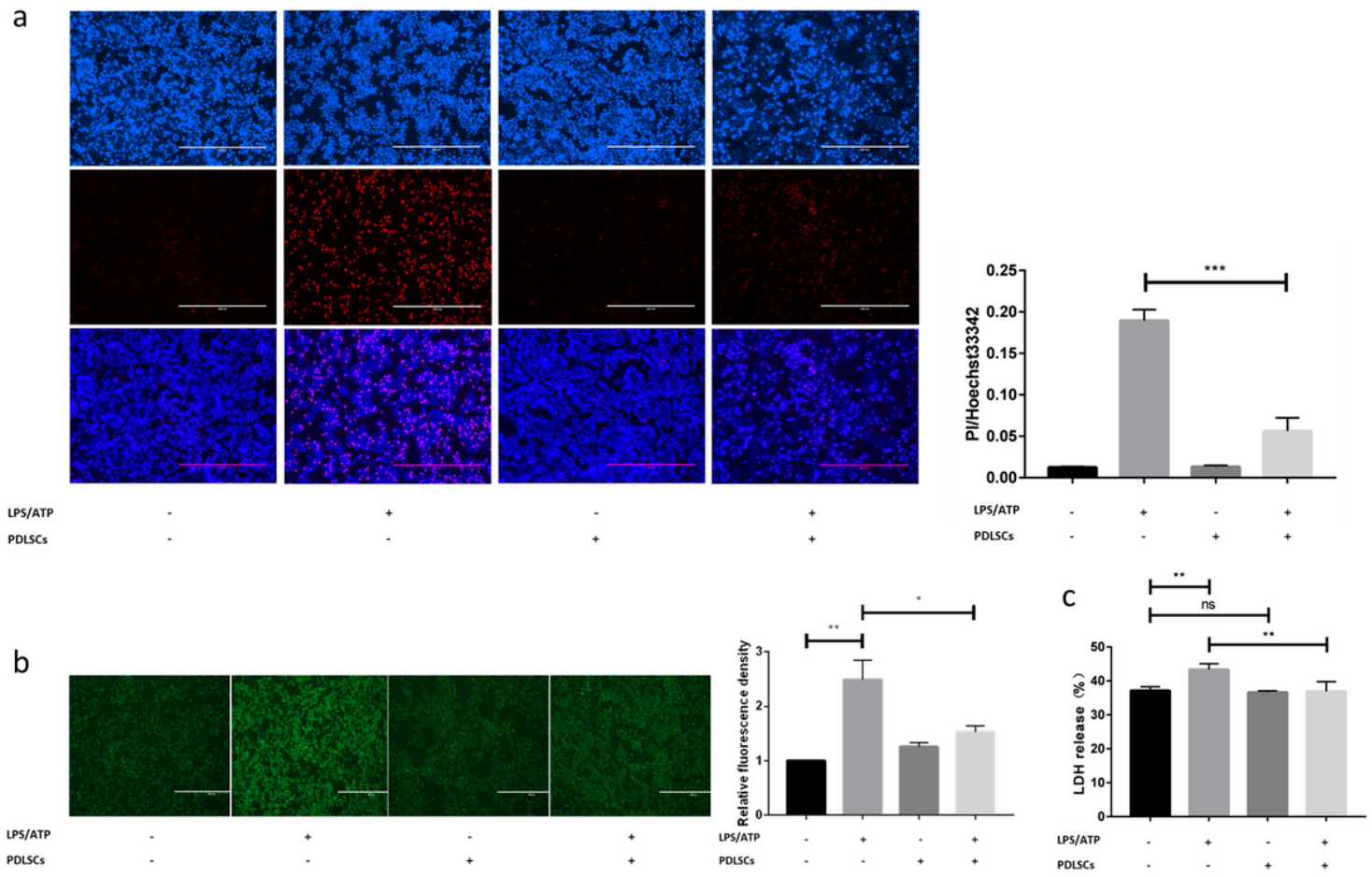

Figure 6

(a)Hoechst 33342 and PI double staining images were captured by fluorescence microscopy (×10), the images in red and blue channels were merged in the same field. (b)Cells were stained with the ROS-sensitive fluorescent probe 2 ,7 -dichlo rofluorescein diacetate (DCFH-DA) and observed under a fluorescence microscope (×10). (c)Cytotoxicity was measured by a lactate dehydrogenase (LDH) release assay. One set of representative images of three independent experiments are shown. Results are shown as the mean ± SD (n = 3) (*p < 0.05, **p < 0.01, ***p < 0.001).

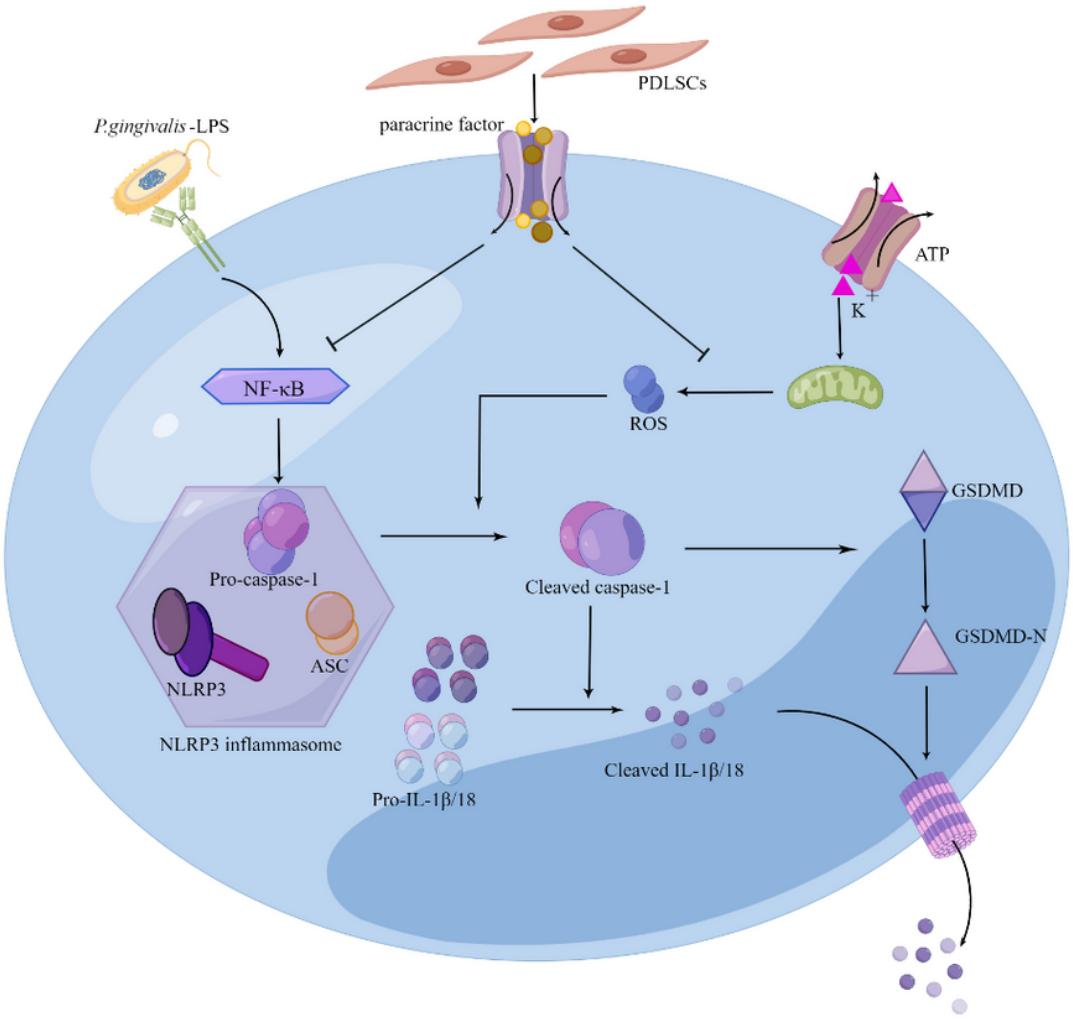

Figure 7

A schematic diagram of the putative molecular mechanism by which paracrine effect of PDLSCs inhibit *P. gingivalis*-LPS/ATP-induced pyroptosis in THP-1 macrophages.